Robust fault detection in hybrid systems using set-membership parameter estimation. ⋆

M. Maïga[1,2], N. Ramdani[1], L. Travé-Massuyès[2]

[1] *Univ. Orléans, INSA-CVL, PRISME, EA 4229, F45072, Orléans, France*
[2] *CNRS, LAAS, University of Toulouse, 31031 Toulouse*
(e-mail: mmaiga@laas.fr, nacim.ramdani@univ-orleans.fr, louise@laas.fr)

Abstract:
Hybrid systems exhibit continuous and discrete dynamics and are encountered in many complex and safety-critical systems. Due to their complex nature, the fault diagnosis task becomes very challenging. In this paper, we present a method to perform fault detection with a nonlinear hybrid system using set-membership parameter estimation in a bounded-error framework. Our method relies on a consistency test between the feasible parameter set as computed in normal fault-free operation or given as nominal, and the feasible parameter set as estimated during on-line operation over a given time horizon. Hence, a fault is detected if the feasible set for the parameter vector estimated online is inconsistent with nominal values. An illustrative example is presented.

Keywords: Bounded error, hybrid systems, interval analysis, nonlinear systems, estimation, reachability, uncertain systems.

1. INTRODUCTION

Nowadays, it is more and more required from current systems to embed capabilities for autonomy that allow them to counteract the occurrence of a fault or any other disturbances, while still providing a reliable functional or degraded service. These systems should contain mechanisms to perceive a degraded operating mode without human intervention, and then perform the necessary corrections for the restoration of a normal operating mode, or a degraded mode but safe. In this framework, a key challenge is to take into account uncertainties. It is essential to consider this incomplete knowledge, which can take in the form of ill-defined disturbances, parameter variations due to a tolerant design, faults, etc. Model-based fault detection and localization methods rely on the detection of discrepancies between the hybrid system outputs and model outputs (see Fig. 1). In the literature there are many model-based fault diagnosis methods available for dynamical systems. For instance, the state estimation approach (Wang et al. (2007); Isermann (1997); Zhao et al. (2005)), the parity space approach (Shumsky and Zhirabok (2012); Bayoudh et al. (2009); Fliss and Tagina (2013)), the parameter estimation approach (Isermann (1993, 1984); Wahrburg and Adamy (2012); Vento et al. (2012)). However, to the best of our knowledge, there is no work to date that investigates set-membership approach to model-based fault detection in the "unknown but bounded error" framework with hybrid dynamic systems (HDS).

In the "unknown but bounded error", all the uncertain quantities (measurement errors, modeling errors and uncertainty) are taken in a bounded set with known bounds. Estimation problems in this framework are then referred to as set-membership estimation. One of the main advantages of the set-membership estimation approach is that it provides a guaranteed decision about fault occurrence, in contrast with the classical notion of risk, usually defined in terms of probability of occurrence and false detection. In other words, these methods allow us to avoid false positive (false alarm). Finally, the contribution of our paper resides in the set-membership fault detection of HDS using a parametric approach, i.e. fault detection relies on the identification of the parameter vector. We have recently proposed an algorithm for performing hybrid reachability (Maïga et al. (2013, 2014)). This algorithm is at the core of the method proposed in this paper. We first define set-membership approach to fault detection with hybrid system, then set membership parameter estimation with hybrid systems, and describe how to build the estimation approach by combining our algorithm for hybrid reachability, and the SIVIA algorithm for set inversion (Jaulin and Walter (1993)) to solving the parameter estimation problem for nonlinear hybrid systems in a bounded-error framework.

The paper is structured as follows: Section 2 formulates the set-membership fault detection, and the parameter estimation problems fo HDS. The set computation tools

⋆ This work is supported by the French National Research Agency under contract ANR 2011 INS 006 MAGIC-SPS (projects.laas.fr/ANR-MAGIC-SPS).

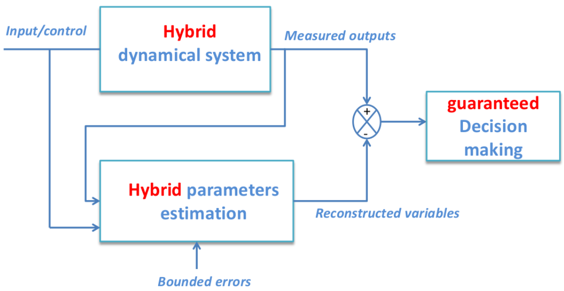

Fig. 1. The monitoring of a hybrid dynamical system in the bounded-error framework

used in the paper are presented in Section 3. Section 4 presents hybrid reachability concepts i.e. interval methods for solving the initial value problem for ordinary differential equation, and the set-membership guard crossing problem. The set-membership fault detection and hybrid parameter estimation will be presented in Section 5. Section 6 gathers experimental evaluation on hybrid mass-spring system.

2. PROBLEM STATEMENT : SET-MEMBERSHIP FAULT DETECTION

Considering the hybrid system is modeled as a hybrid automaton which is defined as in (Alur et al. (1995)) :

$$HA = (\mathbb{Q}, \mathbb{D}, \mathbb{P}, \Sigma, \mathbb{A}, \mathrm{Inv}, \mathbb{F}), \quad (1)$$

- $\mathcal{Q}$ is a set of locations $\{q\}$ whose continuous dynamics, i.e. flow transitions, are described by non-autonomous differential equations $f_q \in \mathcal{F}$ of the form :
$$\mathrm{flow}(q): \quad \dot{x}(t) = f_q(x, p, t), \quad (2)$$
where $f_q : \mathcal{D} \times \mathcal{P} \times \mathbb{R}^+ \mapsto \mathcal{D}$ is nonlinear and assumed sufficiently smooth over $\mathcal{D} \subseteq \mathbb{R}^n$, with dimension n that may depend on q, and $p \in \mathcal{P}$, where $\mathcal{P}$ is an uncertainty domain for the parameter vector p.
- Inv is an invariant, which assigns a domain to the continuous state space of each location:
$$\mathrm{Inv}(q): \quad \nu_q(x(t), p, t) < 0, \quad (3)$$
where inequalities are taken componentwise, $\nu_q : \mathcal{D} \times \mathcal{P} \times \mathbb{R}^+ \mapsto \mathbb{R}^m$ is also nonlinear, and the number m of inequalities may also depend on q.
- $\mathcal{A}$ is the set of discrete transitions $\{e = (q \to q')\}$ given by the 5-uple $(q, \mathrm{guard}, \sigma, \rho, q')$, where q and q' represent upstream and downstream locations respectively; guard is a condition of the form :
$$\mathrm{guard}(e): \quad \gamma_e(x(t), p, t) = 0; \quad (4)$$
σ is an event, and ρ is a reset function assumed to be affine.

A transition $q \to q'$ may occur when the continuous state flow reaches the guard set, i.e. when the continuous state satisfies condition (4). Introducing the new state variable $z = (x, p, t)$ with $\dot{z} = (\dot{x}, 0, 1)$, and defining $\mathcal{Z} = \mathcal{D} \times \mathcal{P} \times \mathbb{R}^+$, equations (2–4) are rewritten :

$$\mathrm{flow}(q): \quad \dot{z}(t) = f_q(z), \quad (5)$$
$$\mathrm{Inv}(q): \quad \nu_q(z(t)) < 0, \quad (6)$$
$$\mathrm{guard}(e): \quad \gamma_e(z(t)) = 0. \quad (7)$$

so that all uncertain quantities are embedded in the initial state vector.

Let us also consider the following measurement equation

$$y(t) = g_q(x, \mathbf{p}, t) \quad (8)$$

where function $g_q : \mathcal{D} \times \mathcal{P} \times \mathbb{R}^+ \mapsto \mathcal{D}$ is nonlinear.

2.1 Set-membership parameter estimation

We assume that measurements $\hat{y}_j$ of the output vector are available at sampling times $t_j \in \{t_1, t_2, ..., T_n\} \subset [t_0, T_{end}]$. Note that the sampling interval need not be constant. The measurement noise is a discrete time signal assumed additive and bounded with known bounds. Denote by $\mathbb{E}_j$ a feasible domain for the output error at time t_j : the feasible domain for the model output at time t_j is then given by :

$$\mathbb{Y}_j = \hat{y}_j + \mathbb{E}_j \quad (9)$$

Given the hybrid model (1-4), the measurements and error bounds, the goal of this paper consists to estimate the parameter vector $\mathbf{p}$ by determining the set $\mathbb{S}$ of all acceptable parameters

$$\begin{aligned}\mathbb{S} = \{\mathbf{p} \in \mathbb{P}_0 | (\forall t \in [t_0, T_{end}],\\ flow(q) \wedge Inv(q) \wedge guard(e)\\ \wedge (\forall t_j \in \{t_1, t_2, ..., T_n\}, g_q(x, \mathbf{p}, t) \in \mathbb{Y}_j\} \quad (10)\end{aligned}$$

where the set $\mathbb{P}_0$ is the initial search space for the parameters. The characterization of the solution set $\mathbb{S}$ is a *set inversion problem* i.e. starting from the set $\mathbb{Y}$, we want to reconstruct the original set $\mathbb{S}$.

2.2 Set-membership fault detection

In the literature (e.g. Guerra and Puig (2008)), fault detection is usually performed either using a “direct” or an “inverse” test. The direct test relies on a worst-case estimation approach whereas the inverse test relies on set-membership estimation approaches, a framework similar to the one investigated in this paper (Blesa et al. (2011, 2012)).

The direct test is based on the evaluation of the residual obtained from the difference between measurements (8) and the output of the hybrid model (1-4) at every instant t_j :

$$r_j = y_j - \hat{y}_j \quad (11)$$

Ideally, when neither modelling errors nor noise are present, the residual given by Eq (11), known also as parity equation, should be different from zero in a faulty scenario and zero otherwise. However, because of modelling and measurement errors and uncertainty, one can derive a feasible domain for the residuals, and the detection test now relies on checking the following condition assuming parametric uncertainty, i.e. $0 \notin \Gamma_j$, where Γ_j is the set of possible residuals considering parameter uncertainties and an additive bounded noise, $\Gamma_j = \{r_j | r_j = y_j - \hat{y}_j + \epsilon_j \text{ and } \epsilon_j \in \mathbb{E}_j\}$.

In the inverse test, the fault detection process is done by estimating the value of model parameters using system identification procedures, and comparing these estimated values to nominal ones (hence assumed known). The difference between these values forms also a residual (Isermann (1993)), which can be written as

$$r_j = p_n - p \quad (12)$$

Here we use a set-membership extension of the inverse test as follows using $\mathbb{S}$ given by Eq (10) and $\mathbb{P}_N$ denoting the set of nominal parameter values.

(1) First $\mathbb{P}_N$ is estimated with nonfaulty data,
(2) during operation, set $\mathbb{S}$ as given by (10) is estimated from running data (possibly containing faults) over a given horizon, and
(3) the intersection $\mathbb{S} \cap \mathbb{P}_N$ is computed,
(4) a fault is detected if $\mathbb{S} \cap \mathbb{P}_N = \emptyset$, which means that the nominal parameter values cannot explain the actual data while considering error bounds ; actual data and the model are inconsistant hence there should be a fault.

Our method for fault detection with hybrid system relies on a new method for set-membership parameter estimation. It uses interval analysis (Moore (1996)), zonotope enclosures (Alamo et al. (2005)) and set inversion (Jaulin and Walter (1993)). It relies also on a new approach to hybrid reachability that is described briefly in next section.

3. HYBRID REACHABILITY

3.1 Continuous transitions

Our validated ODE solvers are based on a three-stage Taylor series approach. The first stage of a Taylor series based verify the existence and uniqueness of the solution using the Banach fixed point theorem and the Picard-Lindelöf operator (Moore (1996)). The second stage consist to compute an a priori enclosure $[\widetilde{\boldsymbol{z}}_j]$ such that $[\widetilde{\boldsymbol{z}}_j] \supseteq \mathcal{Z}(t)$ for all t in $[t_j, t_{j+1}]$. Hence, $[\widetilde{\boldsymbol{z}}_j]$ is indeed an over-approximation of the reachable set over $[t_j, t_{j+1}]$. The third stage of a Taylor series method uses compute a tighter enclosure for the set of solutions of (5) at t_{j+1} using a Taylor series expansion of order k of the solution at t_j, where $[\widetilde{\boldsymbol{z}}_j]$ is used to enclose the remainder term:

$$\mathcal{Z}(t; t_j, \boldsymbol{z}_j) \subseteq [\boldsymbol{z}](t; t_j, [\boldsymbol{z}_j]) = \\ [\boldsymbol{z}_j] + \sum_{i=1}^{k-1} (t - t_j)^i \mathsf{f}_q^{[i]}([\boldsymbol{z}_j]) + (t - t_j)^k \mathsf{f}_q^{[k]}([\widetilde{\boldsymbol{z}}_j]), \quad (13)$$

where t can be taken as t_{j+1} or any $t \in [t_j, t_{j+1}]$, which is not necessarily on the time-grid, and the $\mathsf{f}_q^{[i]}([\boldsymbol{z}_j])$ are the Taylor coefficients. In (Nedialkov et al. (1999)), (13) is turned into a computationally acceptable scheme that controls the wrapping effect [1] by using the *mean-value* approach complemented by QR-factorization as proposed by Lohner. The solution enclosure at time $t \in [t_j, t_{j+1}]$ can be computed in the form mean-value:

$$\mathcal{Z}(t; t_j, \mathcal{Z}_0) \in \{v(t) + A(t)r(t) \,|\, v(t) \in [\boldsymbol{v}](t), r(t) \in [\boldsymbol{r}](t)\}, \quad (14)$$

Defining : $[\boldsymbol{\chi}](t) \equiv \{[\boldsymbol{z}](t),\, \hat{z}(t),\, [\boldsymbol{v}](t),\, [\boldsymbol{r}](t),\, A(t)\}$, where $\hat{z}(t) := \mathrm{Mid}([\boldsymbol{z}](t))$, the algorithm $\varphi^{l_{qr}}(.)$ is used in this paper to compute the solution set of (5) at time $t \in [t_j,\, t_{j+1}]$. It is the same as the one developed in (Maïga et al. (2013)). The solution enclosure at time t_{j+1} is given by $[\boldsymbol{\chi}_{j+1}] = \varphi^{l_{qr}}([\boldsymbol{\chi}_j],\, t_j,\, t_{j+1},\, [\widetilde{\boldsymbol{z}}_j])$.

[1] The wrapping effect is the over-approximation induced by enclosing a set of any shape in an axis-aligned box.

Proposition 1. The solution domain (14) is the Minkowski sum [2] of a parallelotope, i.e. an oriented box, and an aligned box, abbreviated as an MSPB. $\mathbb{Z}(t) = A(t)[r](t) \oplus [v](t)$. An MSPB is a particular zonotope generated by $2n$ line segments: $\mathbb{Z}(t) = c(t) \oplus R(t)\boldsymbol{B}^{2n}$, where, for all t, the point vector $c(t) \in \mathbb{R}^n$ and the point matrix $R(t) \in \mathbb{R}^{n \times 2n}$ satisfy: $c(t) = A(t)\mathrm{mid}\,([r](t)) + \mathrm{mid}\,([v](t))$, and $R(t) = [A(t)\mathrm{dr}\,([r](t)) \mid \mathrm{dr}\,([v](t))]$, where $\mid$ denotes matrix concatenation, and $\mathrm{dr}\,(.)$ is short for $\mathrm{diag}(\mathrm{rad}\,(.))$, i.e. a diagonal matrix of real numbers each corresponding to the radius of an interval number.

3.2 Discrete transitions

We first consider event detection and localization stages. In our previous work (Ramdani and Nedialkov, 2011), given Algorithm $\varphi^{l_{qr}}(.)$, detecting and localizing hybrid transition is shown to be equivalent to finding the set $[\underline{t}^\star,\, \overline{t}^\star] \times \mathcal{Z}_j^\star$, where $\mathcal{Z}_j^\star$ is the initial set consisting of the initial state vectors $z_j^\star$ that lead to a $z(t_e; t_j, z_j^\star)$ that satisfies (7) at t_e and $t_e \in [\underline{t}^\star,\, \overline{t}^\star]$. Accounting for the mean value form introduced in section 3.1, finding such set is performed by solving the following CSP:

$$\big([t_j, t_{j+1}] \times \boldsymbol{r}_j,\, \text{`}\gamma_e\big(\varphi(\chi_j(.), ., t, .)\big) = 0\text{'}\big)\,. \quad (15)$$

If the set $[\underline{t}^\star, \overline{t}^\star] \times [\boldsymbol{r}_j^\star]$ is not empty, one can assume that the event $e = q \to q'$ occurs at $t_e = \underline{t}^\star$ and that $[\boldsymbol{\chi}](t_e^-) = [\boldsymbol{\chi}]([\underline{t}^\star, \overline{t}^\star]$. The discrete transition can then be computed from $[z(t_e^-)]$ thanks to the reset function ρ. (Ramdani and Nedialkov (2011)) enhances the method by proposing a bisection strategy that account for the size of $[\underline{t}^\star,\, \overline{t}^\star]$ and $[\mathcal{Z}_j^\star]$. We use a conservative relaxation of the above algorithm as described in (Maïga et al. (2013, 2014)) : in fact, we do not search all initial state vectors that lead the flow to satisfy the guard condition, but we merely compute the a priori solution $[\widetilde{\boldsymbol{z}}]$, i.e. an enclosure of the reachable set over the time interval $[t_0, t_1]$. Having determined $[\boldsymbol{\chi}_{j+1}]$, (Ramdani and Nedialkov (2011)) proposes to compute the flow/invariant intersection at time t_{j+1} by solving the following CSP:

$$([\boldsymbol{v}_{j+1}] \times [\boldsymbol{r}_{j+1}],\, \text{`}\nu_q([v_{j+1}] + A_{j+1}[r_{j+1}]) < 0\text{'}). \quad (16)$$

If $[\boldsymbol{v}_{j+1}]' \times [\boldsymbol{r}_{j+1}]'$ is the solution set of CSP (16), then the solution set $[\boldsymbol{z}_{j+1}]' = \mathrm{inv}(q) \cap [\boldsymbol{z}_{j+1}]$ is given by:

$$[\boldsymbol{z}_{j+1}]' = \{v_{j+1} + A_{j+1} r_{j+1},\, |\, v_{j+1} \in [\boldsymbol{v}_{j+1}]',\, r_{j+1} \in [\boldsymbol{r}_{j+1}]'\}.$$

4. OUR METHOD FOR PARAMETER ESTIMATION

4.1 Set-membership parameter estimation

We address set-membership estimation of the parameter vector of the hybrid system (1-4), i.e. the computation of set (10) by extending SIVIA set inversion via interval analysis (Jaulin and Walter (1993)) to hybrid systems. Though SIVIA was initially introduced for closed-form models, it can be extended to differential or hybrid dynamical models as long as one can obtain conservative numerical evaluation of the solution set $[x_j]$ of (1-4) at measurement time instants t_j. This evaluation can be obtained using our hybrid reachability method recalled in section 3. The

[2] Let $\xi_1, \xi_2 \subset \mathbb{R}^n$, the Minkowski sum of ξ_1 and ξ_2 is: $\xi_1 \oplus \xi_2 = \{s_1 + s_2 |\, s_1 \in \xi_1, s_2 \in \xi_2\}$.

Algorithm 1: Algorithm `Parameter estimation with hybrid systems`

input : $[p], T_{end}, \Delta_T, hybrid\_reach(), F_{(1:n)}, R_{(1:n)}, \mathcal{L}_m, \epsilon$
output: $\mathcal{L}_a, \mathcal{L}_r, \mathcal{L}_i$
$\mathcal{L}_c \leftarrow [p]$, $n := \frac{T_{end}}{\Delta_T} + 1$;
while $\mathcal{L}_c \neq \emptyset$ **do**
  $inclusion := 0$; $[p] := pop(\mathcal{L}_c)$;
  `/* Compute hybrid reachable set over whole horizon` T_{end} `*/`
  $(F_{(1:n)}, R_{(1:n)}) \leftarrow hybrid\_reach([p], \Delta_T, T_{end})$;
  for $j = 1$ *to* n **do**
    `/*` F_j`, Frontier at` t_j `*/`
    $test \leftarrow$**Inclusion-Test**$(F_j, \mathcal{L}_m(j))$;
    if $(test == false)$ **then**
      break;
    else if $(test == true)$ **then**
      $inclusion := inclusion + 1$;
    end if
  end for
  if $(test == false)$ **then**
    $\mathcal{L}_r \leftarrow [p]$;
  else
    if $(inclusion == n)$ **then**
      $\mathcal{L}_a \leftarrow [p]$;
    else if $w([p]) \leq \epsilon$ **then**
      $\mathcal{L}_i \leftarrow [p]$;
    else
      $\{[p]_l, [p]_r\} :=$ **Partition**$([p])$;
      $\mathcal{L}_c \leftarrow [p]_l$; $\mathcal{L}_c \leftarrow [p]_r$;
    end if
    end if
  end if
  end if
end while

extension of SIVIA algorithm to hybrid dynamical systems is gathered in Algorithm 1. It allows us to partition the initial bounded search space for the parameters $\mathbb{P} = [\mathbf{p}]$ and to compute two subsets : an inner approximation $\underline{\mathbb{S}}$ and an uncertainty layer $\Delta\mathbb{S}$, such that $\underline{\mathbb{S}} \subseteq \mathbb{S} \subseteq \underline{\mathbb{S}} \cup \Delta\mathbb{S}$. If $\mathbb{P}$ is too uncertain, it might be necessary to partition $\mathbb{P}$ and iteratively apply SIVIA to every box of the partition. An alternative method is proposed in Travé-Massuyès et al. (2015) based on a *Focused Recursive Partition.* In order to extend SIVIA, we only have to define the inclusion test for the hybrid dynamical system. In this paper we propose Algorithm 2, which checks if a union of zonotopes is included in the feasible domain for measurements.

4.2 Checking inclusion test using a union of zonotopes

Proposition 1. Given a zonotope Z and a strip $\mathcal{S} = |\eta^\top x - d| \leq \sigma$, the zonotope support strip (Vicino and Zappa (1996)) is defined by $\mathcal{S}_\mathsf{Z} = \{x \in \mathbb{R}^n | q_d \leq \eta^\top x \leq q_u\}$, where q_u and q_d are defined as $q_u = \max_{x \in \mathsf{Z}} \eta^\top x$, and $q_d = \min_{x \in \mathsf{Z}} \eta^\top x$. They are easily computed by $q_u = \eta^\top c + \|R^\top \eta\|_1$ and $q_d = \eta^\top c - \|R^\top \eta\|_1$ where $\|.\|$ is the 1-norm of a vector.

Theorem 1. ((Vicino and Zappa (1996))). The zonotope $\mathsf{Z} = c \oplus R\boldsymbol{B}^p \in \mathbb{R}^n$ is included in the strip $\mathcal{S}_j = |\eta^\top x - d| \leq \sigma$ related to measurement datum $[y_j]$ iff $(q_d \geq d_j - \sigma_j) \wedge (q_u \leq d_j + \sigma_j)$ where $d_j = \text{mid}\,([y_j])$, $\sigma_j = \text{rad}([y_j])$

Algorithm 2: `Inclusion-Test`

input : F_j, y_j
output: $true, false, uncertain$
`/* Inclusion test between frontier` F_j `and datum` y_j `at time instant` t_j `*/`
inclus:=0; nointer:=0;
for $l = 1$ *to length*(Fj) **do**
  $\{A_l^j, [r_l^j], [v_l^j]\} := pop(F_j)$;
  $\mathsf{Z}_l^j :=$ `Box2zonotope`$(A_l^j, [r_l^j], [v_l^j])$;
  $\mathsf{Z}_l^{j\star} := g([Z_l^j])$;
  $\mathcal{S}_j \leftarrow \{\eta, d_j = \text{mid}\,([y_j]), \sigma_j = rad([y_j])\}$;
  if $\forall l \left(\mathsf{Z}_l^{j\star} \subseteq \mathcal{S}_j\right)$ **then**
    inclus++;
  end if
  if $\left(\mathsf{Z}_l^{j\star} \cap \mathcal{S}_j == \emptyset\right)$ **then**
    nointer++;
  end if
end for
if *(inclus==length*(Fj)) **then**
  return true;
end if
if *nointer* > 0 **then**
  return false;
end if
return ambiguous;

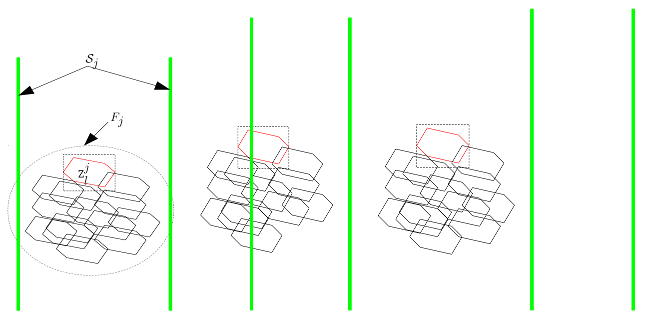

(a) Test: is `true` (b) is `ambiguous` (c) is `false`

Fig. 2. Inclusion test outcomes with zonotopes for frontier list F_j at time t_j

Theorem 2. ((Vicino and Zappa (1996))). The zonotope $\mathsf{Z} = c \oplus R\boldsymbol{B}^p \in \mathbb{R}^n$ do not intersect the strip $\mathcal{S}_j = |\eta^\top x - d| \leq \sigma$ iff $(q_d > d_j + \sigma_j) \vee (q_u < d_j - \sigma_j)$ where $d_j = \text{mid}\,([y_j])$, $\sigma_j = \text{rad}([y_j])$

4.3 SIVIA-H : SIVIA for hybrid systems

Our algorithm (Algorithm 1) generates three lists $\mathcal{L}_a, \mathcal{L}_r, \mathcal{L}_i$. The first list $\mathcal{L}_a$ contains subpaving $[\mathbf{p_i}] \subset [\mathbf{p}]$ which yields an inclusion test as true (see Fig.2-b), i.e:

$$\forall t_j \in \{t_1, t_2, ..., T_n\}, l = 1, 2, \ldots, length(F_j), flow(q) \wedge Inv(q) \wedge guard(e) \wedge g_q([x_l^j], [\mathbf{p_i}]) \in \mathbb{Y}_j \quad (17)$$

The union of subpavings as given by the first list $\mathcal{L}_a$ characterizes an inner approximation $\underline{\mathbb{S}}$ of set $\mathbb{S}$. The second list $\mathcal{L}_r$ consists of all subpaving which the inclusion test is false (see Fig.2-d) i.e. the subpaving for which the structure of the model, the experimental data, and the error bounds are inconsistent, i.e.:

$$\exists t_j \in \{t_1, t_2, ..., T_n\}, l = 1, 2, \ldots, length(F_j), flow(q) \\ \wedge Inv(q) \wedge guard(e) \wedge g_q([x_l^j], [\mathbf{p_i}]) \cap \mathbb{Y}_j = \emptyset \quad (18)$$

where F_j is the frontier (i.e. the subpaving of solution boxes) at instant t_j and $[x_l^j] = F_j(l)$ a solution box of the frontier F_j with $l = 1, 2, \ldots, length(F_j)$. When one cannot conclude about the outcome of the inclusion test, i.e. neither condition (17) nor condition (18) are satisfied, algorithm *SIVIA-H* bisects the parameter boxes under study and then performed the test again. The choice of the bisection direction is based for example on the size of the box subpaving to partition (Jaulin and Walter (1993)). We repeat this process until the size of the box under analysis reaches a threshold ϵ chosen by the user. Finally, the third list, denoted $\mathcal{L}_i$, contains all the undetermined boxes which size is smaller than ϵ.

To summarize, the principle of our approach for set membership parameter identification for hybrid systems, we consider first a parameter box $[\mathbf{p_i}]$, for which we compute the whole hybrid reachable set over $[t_0, t_{end}]$, thanks to our hybrid reachability algorithm (Maïga et al. (2013, 2014)). Then if condition (17) is satisfied, i.e. the parameter box is consistent with the measurements, we add the box to list $\mathcal{L}_a$ to form the inner approximation. To the contrary, if condition (18) is satisfied, i.e. the parameter box is not consistent with the measurements, the model structure and the error bounds, this parameter box is added to the list $\mathcal{L}_r$, i.e. the rejected boxes. Now, if the two conditions are not satisfied and the size of the subpaving is less than the threshold ϵ, the parameter box is then added to the list $\mathcal{L}_i$, to form the uncertainty layer.

5. NUMERICAL EVALUATION

For the purpose of numerical experimentation, the above system-solving methods have been implemented in the `IBEX` C++ library (www.ibex-lib.org) and we have used the standard contractor `HC4Revise` it includes. We have also used `Profil/Bias` C++ class library for interval computation, `FABDAB++` package (www.fadbad.com) for automatic differentiation and computing the Taylor coefficients, `AML++` (amlpp.sourceforge.net) and `Armadillo` (arma.sourceforge.net) package for Linear algebra. All experiments were tested on a $i5-2430$M 2.4GHz CPU with 3.8GB RAM running Ubuntu Linux.

5.1 Example : A hybrid mass-spring system

Consider the mass-spring system with three modes of operation $q = 1$, 2, 3 and four transitions given by :

$$\begin{cases} \text{flow}(1): f_1(x_1, x_2) = \left(x_2, \frac{-k}{m}x_1 - \frac{c}{m}x_2\right) \\ \text{inv}(1): \nu_1(x_1, x_2) = x_2 \geq -v_0 \\ \text{guard}(1): \gamma_1(x_1, x_2) = x_2 < -v_0 \\ \text{reset}(1): \rho_1(x_1, x_2) = (\alpha_1 x_1, \alpha_2 x_2) \\ \text{flow}(2): f_2(x_1, x_2) = \left(x_2, \frac{-k}{m}x_1 - \frac{c}{m}x_2\right) \\ \text{inv}(2): \nu_2(x_1, x_2) = x_2 \leq -v_0 \wedge x_2 \geq v_0 \\ \text{guard}(2): \gamma_1(x_1, x_2) = x_2 \leq v_0 \\ \text{reset}(2): \rho_1(x_1, x_2) = (\alpha_1 x_1, \alpha_2 x_2) \\ \text{flow}(3): f_1(x_1, x_2) = \left(x_2, \frac{-k}{m}x_1 - \frac{c}{m}x_2\right) \\ \text{inv}(3): \nu_1(x_1, x_2) = x_2 \leq v_0 \\ \text{reset}(3): \rho_1(x_1, x_2) = (\alpha_1 x_1, \alpha_2 x_2) \end{cases} \quad (19)$$

The continuous states are described by two variables (x_1, x_2), where x_1, x_2 represents respectively the position and the velocity of the mass. $\alpha_1 = \alpha_2 = 1$. The integration step is chosen constant $h = 0.1$ in the ODE solver. The time variable is bisected until the treshold $\varepsilon_T = 0.005$. To illustrate the performance of our approach we consider two case-studies. In the first one, we will identify $p_1 = \frac{k}{m}$ and $p_2 = \frac{c}{m}$ assuming $p_3 = v_0$ known. In the second one, we will identify $p_1 = \frac{k}{m}$ and $p_3 = v_0$ assuming $p_2 = \frac{c}{m}$ is known.

The mass-spring system operates as follows : first we start in mode q_1 (Fig. 3) with the damper disconnected i.e. $c_1 = 0$, then when velocity x_2 exceeds a given threshold v_0 ($|\dot{x}_2| \geq v_0$), the system connects the damper $c_2 \neq 0$ and the system switches to mode q_2. Starting from mode q_2, when the velocity is below the threshold v_0 ($|\dot{x}_2| < v_0$), the damper is disconnected and the system moves back to mode q_1 and so on. We measure the position of the mass. We have 45 possible measurements of the position over the whole time horizon $T_{end} = 4.4s$, but to illustrate the robustness of our approach, only 12 measurements have been chosen. Initial conditions for state vectors are known with good precision: $x_1 \in [1, 1.1]$, $x_2 \in [0.1, 0.1]$. Artificial data are gathered with the parameter vector $\mathbf{p}^\star = (2.1 \times 0.63 \times 0.5)$ and the assumption on noise bounds are $\mathbb{E}_j = [-0.01, 0.01]$. The initial search box is taken as $[\mathbb{P}_0] = [1.5; 3] \times [0; 1.5]$ for the first case-study and $[\mathbb{P}_0] = [1.5; 3] \times [0.35; 0.65]$ for the second case-study. $\epsilon = 0.01$.

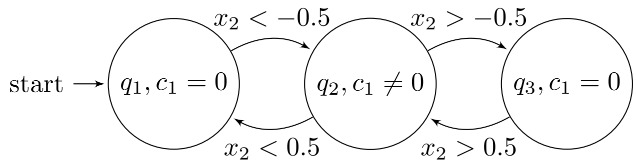

Fig. 3. The hybrid automata for the mass-spring system under study

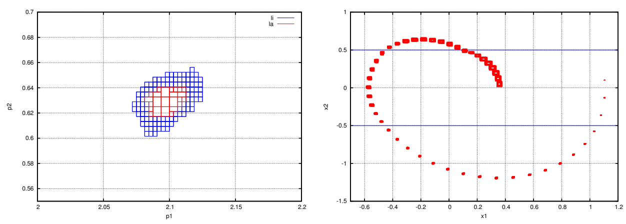

Fig. 4. Solution set in parameters space $p_2 \times p_1$, and reachable set, for case study 1. Left:Inner approximation(red boxes), uncertainty layer (blue boxes). Right: Reachable set on the phase plan $x_2 \times x_1$.

Case study 1. The inner and the uncertainty layers approximations are depicted in Fig. 4 for the parameter space $p_2 \times p_1$. We have also plotted the reachable set in phase plan $(x_2 \times x_1)$ i.e. velocity vs position for all parameters that are consistent with the measurements Fig. 4.

Case study 2. The inner and uncertainty layer approximations are depicted in Fig. 5 for the parameter space $p_3 \times p_1$. We have also plotted the reachable set in phase plan $(x_2 \times x_1)$ i.e. velocity vs position for all parameters vectors

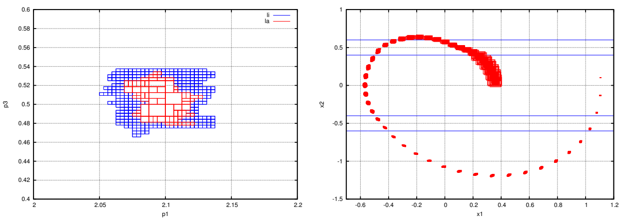

Fig. 5. Solution set in parameters space $p_3 \times p_1$, and reachable set, for case study 2. Left:Inner approximation(red boxes), uncertainty layer (blue boxes). Right: Reachable set on the phase plan $x_2 \times x_1$.

that are consistent with the measurements Fig. 5. These figures clearly show that our approach can solve in a very natural way the problem of set-membership estimation of the parameters driving discrete transitions in hybrid systems, i.e. the identification of the guard or switching hyper-surface of the nonlinear dynamical system.

6. CONCLUSION

This paper has addressed the problem of set-membership estimation and fault detection for nonlinear hybrid system in a bounded-error framework. For set-membership parameter estimation, we have shown how to extend the classical set inversion via interval analysis to hybrid dynamical systems using our algorithm for hybrid reachability. The latter makes it possible to build the inclusion test used within our now new algorithm SIVIA-H. Fault detection relies on the "inverse" test, i.e. compares the feasible parameter set estimated on the running data with nominal parameter values. The evaluation performed shows nice results for the parameter estimation. Future work will consolidate the use of our parameter estimation for fault detection and diagnosis of hybrid systems.

REFERENCES

Alamo, T., Bravo, J., and Camacho, E. (2005). Guaranteed state estimation by zonotopes. *Automatica*, 41, 1035–1043.

Alur, R., Courcoubetis, C., Halbwachs, N., Henzinger, T.A., Ho, P.H., Nicollin, X., Olivero, A., Sifakis, J., and Yovine, S. (1995). The algorithmic analysis of hybrid systems. *Theoretical Computer Science*, 138, 3–34.

Bayoudh, M., Trave-Massuyes, L., and Olive, X. (2009). On-line analytic redundancy relations instantiation guided by component discrete-dynamics for a class of non-linear hybrid systems. In *IEEE CDC/CCC*, 6970–6975.

Blesa, J., Puig, V., and Saludes, J. (2011). Identification for passive robust fault detection using zonotope-based set-membership approaches. *International Journal of Adaptive Control and Signal Processing*, 25(9), 788–812.

Blesa, J., Puig, V., and Saludes, J. (2012). Robust identification and fault diagnosis based on uncertain multiple input–multiple output linear parameter varying parity equations and zonotopes. *Journal of Process Control*, 22(10), 1890–1912.

Fliss, I. and Tagina, M. (2013). Diagnosing multiple faults in dynamic hybrid systems. In A. Abraham and S.M. Thampi (eds.), *Intelligent Informatics*, volume 182 of *Advances in Intelligent Systems and Computing*, 129–139. Springer Berlin Heidelberg.

Guerra, P. and Puig, V. (2008). Passive robust fault detection using interval ma parity equations: inverse vs direct image tests. In *IFAC World Congress, Seoul.*

Isermann, R. (1984). Process fault detection based on modeling and estimation methods-a survey. *Automatica*, 20(4), 387–404.

Isermann, R. (1993). Fault diagnosis of machines via parameter estimation and knowledge processing: Tutorial paper. *Automatica*, 29(4), 815–835.

Isermann, R. (1997). Supervision, fault-detection and fault-diagnosis methodsan introduction. *Control engineering practice*, 5(5), 639–652.

Jaulin, L. and Walter, E. (1993). Set inversion via interval analysis for nonlinear bounded-error estimation. *Automatica*, 29, 1053–1064.

Maïga, M., Ramdani, N., and Travé-Massuyès (2014). A CSP versus a zonotope-based method for solving guard set intersection in nonlinear hybrid reachability. *Mathematics in Computer Science*, 8(3-4).

Maïga, M., Ramdani, N., and Travé-Massuyès, L. (2013). A fast method for solving guard set intersection in nonlinear hybrid reachability. In *IEEE CDC 2013.*, 508–513.

Moore, R.E. (1996). *Interval Analysis*. Englewood Cliffs, prentice-hall.

Nedialkov, N., Jackson1, K., and Corliss, G. (1999). Validated solutions of initial value problems for ordinary differential equations. *Applied Mathematics and Computation*, 105(1), 21 – 68.

Ramdani, N. and Nedialkov, N.S. (2011). Computing reachable sets for uncertain nonlinear hybrid systems using interval constraint-propagation techniques. *Nonlinear Analysis: Hybrid Systems*, 5(2), 149 – 162.

Shumsky, A. and Zhirabok, A.N. (2012). Redundancy relations for fault diagnosis in hybrid systems. In *Fault Detection, Supervision and Safety of Technical Processes*, volume 8, 1226–1231.

Travé-Massuyès, L., Pons, R., Ribot, P., Pencole, Y., and Jauberthie, C. (2015). Condition-based monitoring and prognosis in an error-bounded framework. In *to appear in Proc. 26th Int. Workshop on Principles of Diagnosis, DX'15, Paris, France.*

Vento, J., Puig, V., Sarrate, R., et al. (2012). Fault detection and isolation of hybrid systems using diagnosers that reason on components. In *Fault Detection, Supervision and Safety of Technical Processes*, volume 8, 1250–1255.

Vicino, A. and Zappa, G. (1996). Sequential approximation of feasible parameter sets for identification with set membership uncertainty. *Automatic Control, IEEE Transactions on*, 41(6), 774–785.

Wahrburg, A. and Adamy, J. (2012). Robust fault isolation observers for non-square systems-a parametric approach. In *Fault Detection, Supervision and Safety of Technical Processes*, volume 8, 1275–1280.

Wang, W., Li, L., Zhou, D., and Liu, K. (2007). Robust state estimation and fault diagnosis for uncertain hybrid nonlinear systems. *Nonlinear analysis: Hybrid systems*, 1(1), 2–15.

Zhao, F., Koutsoukos, X., Haussecker, H., Reich, J., and Cheung, P. (2005). Monitoring and fault diagnosis of hybrid systems. *Systems, Man, and Cybernetics, Part B: Cybernetics, IEEE Transactions on*, 35(6), 1225–1240.